Pulsed laser deposition of tungsten-doped diamond-like carbon films

WANG XUEMIN, SHENG CHANGLE, WANG YUYIN, PENG LIPING, WU WEIDONG*, TANG YONGJIAN
Science and Technology on Plasma Physics Laboratory, Research Center of Laser Fusion, China Academy of Engineering Physics, Mianyang, 621900, Sichuan, P. R. China

Tungsten-doped diamond-like carbon films with a total thickness about 300 nm were prepared by pulsed laser deposition (PLD) method on silicon substrates. The properties of these films were examined by X-ray diffractometer (XRD), white light interferometer, Raman spectroscopy and nanoindentation. The presence of obvious broad peaks for diffraction planes (111) indicates the formation of WC_{1-x} phase in the films. Surface morphology confirms the smooth surface of the films (RMS: ~6.36 nm). The behavior of D to G peak intensity ratio has been obtained. It may result from the formation of W-C bonds. Due to the introduction of WC_{1-x} crystallites in the matrix, optimal deposition time of tungsten leads to the highest hardness.

(Received November 29, 2012; accepted April 11, 2013)

Keywords: Coating materials, Laser processing, X-ray diffraction, Mechanical properties

1. Introduction

Carbon-based films are well known for their unusual and promising electrical and optical properties, which show great potential applications in high-power and high-frequency electronic devices, optoelectronic devices and protective coatings [1-4]. The great versatility of Carbon-based materials arises from the strong dependence of their physical properties on the ratio of sp^2 to sp^3 bonds [5] and the doped elements [6,7]. Therefore, over the last years, special attention has been paid to the percentages of sp^3 and sp^2 bonds and the microstructural modification due to the doping of the second elements.

Moreover, during deposition carbon-based films develop high internal compressive stress which prevents their formation as thick films. One efficient method to overcome this drawback is the using of multilayered nanocomposites, which combine desirable properties from their components. W/a-C [8], Mo/a-C [9], TiN/a-C [10], Cr/a-C [11], Al/a-C [12], et al have shown better properties than monolithic a-C films. However, there are a few studies about carbon-based multilayer films. Generally, metal incorporation is known to increase the chemical affinity between the multilayers [13]. The reason of the reduction in stress resulting from metal incorporation is not clear partly due to the varied atomic bonding within the amorphous carbon matrix [14]. On the other hand, different deposition methods such as ion beam, sputtering, cathodic arc, pulsed laser deposition, plasma beam chemical vapour deposition, et al. can prepare various amorphous carbon films. Although, ion bombardment regardless of different deposition methods has been accepted as the main physical process to promote the formation of sp^3 bonds, there is no unanimous deposition mechanism. Thus, the deposition mechanism needs further investigation.

In this work, tungsten-doped diamond-like carbon films have been deposited by pulsed laser deposition (PLD). PLD becomes popular for its simplicity, versatility and capability to generate highly energetic carbon species with high tetrahedral (sp^3) fractions which enhance the synthesis of good mechanical and optical amorphous carbon films. The surface morphologies and structures were characterized by white light interferometer, SEM and XRD. The mechanical property was measured with a Nano Indenter XP system.

2. Experimental details

The experimental details were summarized in Table 1. High purity targets (99.999% pyrolytic graphite and 99.9% tungsten) were used for the ablation experiments with a pulsed KrF excimer laser (COMPexPro®), which provided a beam with 248 nm wavelength, ~4 J pulse energy and 30 ns pulse duration at a repetition rate of 2 Hz [15]. The laser beam was moved in spirals and with constant vector velocity across the target area. The residual gas pressure was $\sim 4\times10^{-5}$ Pa and the deposited temperature was 343 K. Deposition occurred on single crystalline silicon substrates oriented almost parallel to the target at a distance of 5.0 cm. During the deposition process, both tungsten and carbon targets mounted on a rotating holder were alternatively ablated by the pulsed laser beam. The thickness of tungsten layer was controlled by adjusting the deposition time of a cycle for tungsten: 0 min, 5 min, 15 min, 30 min and 60 min for samples 1, 2, 3, 4 and 5 respectively, and the deposition time of a cycle for carbon

was kept to be constant (90 min) for all samples. The average thickness was obtained by α-step profilometer employing a step made using a shadow mask.

Table 1. The experimental parameters for tungsten-doped DLC films.

Working vacuum	~4×10^{-5} Pa
Substrate temperature	~70 °C
Target	Tungsten>99.9% purity, pyrolytic graphite (Kurt J. Lesker)>99.999 purity
Substrate	n-type Si(111) wafer with a thickness of 300±10 μm
Laser fluence	~4 J/cm^2
Laser pulse frequency	2 Hz
The target to substrate distance	5 cm
Number of the cycles for both tungsten and carbon	4
The thickness of the films for samples 1, 2, 3, 4 and 5 respectively	293 nm, 292 nm, 296 nm, 301 nm, 302 nm

An X-ray diffractometer (X Pert PRO) using Cu K_α radiation with an incidence angle of 0.5° (GIXRD) and a scanning resolution of 0.02° was applied to investigate the crystal structure. Raman spectra were recorded by a conventional grating Raman spectrometer (Renishaw Ramanscope) applying an argon ion laser with a wavelength of 514.5 nm in the 800-2000 cm^{-1} range and a resolution of 2 cm^{-1}. The hardness and elastic modulus of the films were measured by nanoindention on MTS Nano Indenter XP with a Berkovich diamond tip.

3. Results and discussion

3.1 Surface morphologies

Typical surface morphologies were examined by white light interferometry and SEM (See Fig. 1). As shown in Fig. 1, the surface of sample 2 is compact and smooth without obvious fluctuation and cracks. In an macro area of 1.2 mm×0.9 mm (Fig. 1 (a)), the root means square roughness (RMS) is about 6.36 nm which is generally in agreements with other results [16]. This means that smooth tungsten-doped diamond-like carbon films can be obtained by PLD method. It indicates the great potential application in tribological fields.

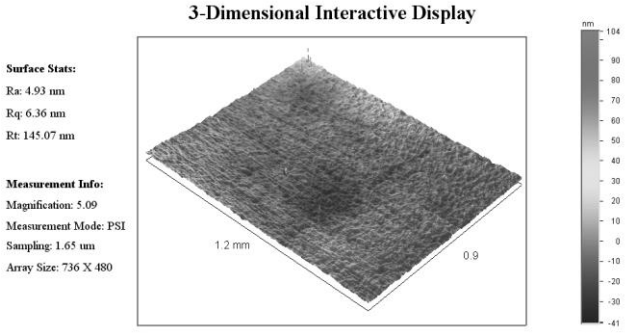

(a)

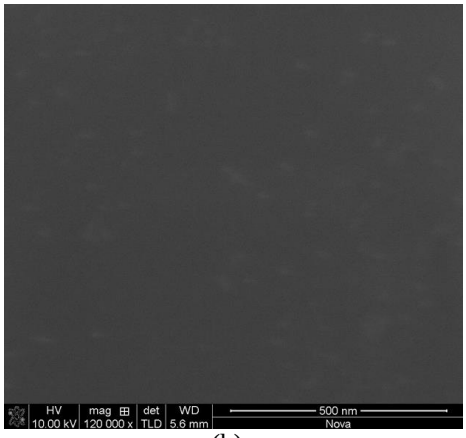

(b)

Fig. 1. Surface morphologies of sample 2: (a) White light interferometry, (b) SEM.

3.2 Structure of the films

The crystalline structures of the tungsten-doped diamond-like carbon films were analyzed by GIXRD. The results were presented in Fig. 2 and shifted upward for easy comparison. Obvious broad peaks for diffraction planes (111) are related with the WC_{1-X} phase, in agreement with other result [17]. The formation of WC_{1-X} phase can be attributed to the implantation of tungsten [18]. In our case, the energy of tungsten ions was assumed from ~40 eV to ~100 eV [2], and tungsten ions were calculated to penetrate from 7 Å to 10 Å into the surface by TRIM code [19]. The instantaneous (10^{-11}-10^{-13} s) high temperature (~10^3 K) and high pressure (~10^9 Pa) in local region [2] can be induced by such an implantation of tungsten ions. Therefore, after this complex process the rapid increase in local density can happen and result in the formation of WC_{1-X} phase as shown in Fig. 2.

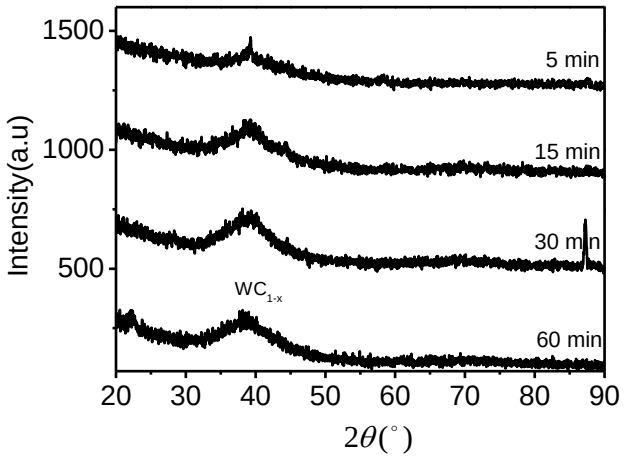

Fig. 2. GIXRD spectra of the deposited tungsten-doped diamond-like carbon films.

3.3 Raman spectroscopy

The Raman spectrum for each sample was obtained using 514 nm excitation and shown in Fig. 3. As indicated in Fig. 3, the Raman spectra are similar and are characterized as a combination of two bands. A G peak at ~1550 cm^{-1} reflects the zone-center E_{2g} mode of a perfect graphite crystal and a D peak at ~1350 cm^{-1} is a zone-edge A_{1g} mode due to the disorder [20]. It is well known that for 514.5 nm excitation the D and G peaks are typically located at 1335 cm^{-1} and in the range of 1580±20 cm^{-1}, respectively. In our case, by deconvoluted into Gaussian D and G peaks by curve-fitting, the D-peak position was found to vary between 1325.8 cm^{-1} and 1409.3 cm^{-1} with the increase of the tungsten deposition time of a cycle. The change of G-peak position is about 18.8 cm^{-1} (1549.6 cm^{-1} for sample 1 to 1568.4 cm^{-1} for sample 2). The upper shift of the G-peak position after tungsten incorporation can be due to the enhanced number of oleofinic sp^2 groups in chains [21]. The full width at half maximum (FWHM) of the G peaks as a function of the deposition time of tungsten were summarized in Fig. 4. It can be seen that the G-peak width of the four tungsten-carbon multilayer films was all lower than that of the bare tungsten incorporated carbon film (sample 1), and exhibited a maximum value for sample 3. Schwan et al. [22] found that the FWHM of G peaks reduces linearly with the decrease of internal stress in the films. Therefore, the reduced stress in the tungsten-incorporated hydrogenated amorphous carbon films may be due to the decreased directionality of the W-C bonds by the distorted bonds [23,24]. The unusual stress behavior can be concluded from the characterization of the G-peak width, as indicated in Fig. 4. Sample 3 with the largest G-peak width, corresponding to the highest sp^3 content, might indicate the highest internal stress in the films. B.R. Pujada, et al found that the huge variation in the compressive stress of tungsten carbide-diamond-like carbon coatings by sputter deposition was due to a change in the microstructure of the coating from polycrystalline to amorphous and not to the energy of positive ions bombarding the film [25]. Therefore, it can be suggested that the internal stress behavior can be due to the decreased directionality of the W-C bonds in the films.

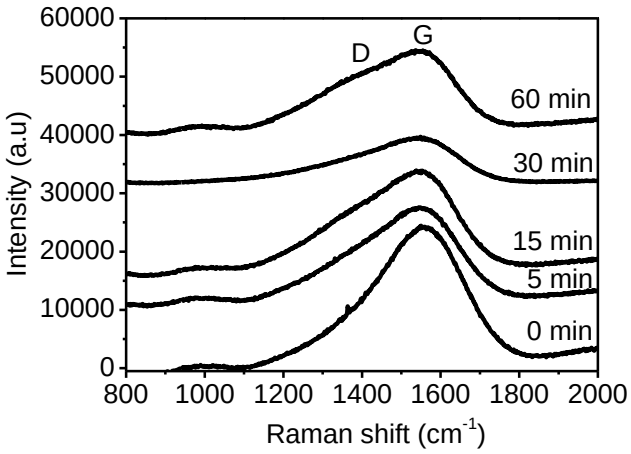

Fig. 3. Visible Raman spectra of the deposited tungsten-doped diamond-like carbon films.

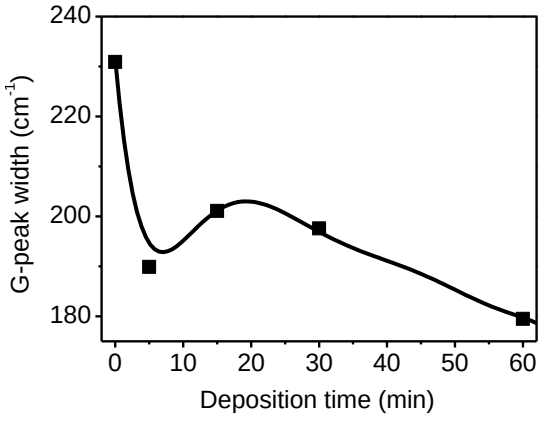

Fig. 4. FWHM of the G peaks as a function of the tungsten deposition time.

It is known that the increase of the relative intensity ratio (I_D/I_G) indicates the state of development of sp^2 phase and the beginning of sp^2 sites to organize into small graphitic clusters [26,27]. Therefore, I_D/I_G is qualitatively related to the sp^3/sp^2 ratio in the carbon-based films. A lower I_D/I_G ratio corresponds to higher sp^3 content. Fig. 5 presents the corresponding I_D/I_G ratio of the tungsten-doped diamond-like carbon films. For all series of tungsten-doped diamond-like carbon films, I_D/I_G shows a complex behavior. Firstly, I_D/I_G of the tungsten-doped diamond-like carbon films are all higher than that of the bare tungsten incorporated carbon film. This means that the sp^3 content seems to reduce after tungsten incorporation, which might be due to the change of carbon states because of the bond angle dispersion [24]. Secondly, I_D/I_G of the tungsten-doped diamond-like carbon films exhibit a minimum value for sample 3, indicating the highest sp^3 content. This is in agreement with the above results.

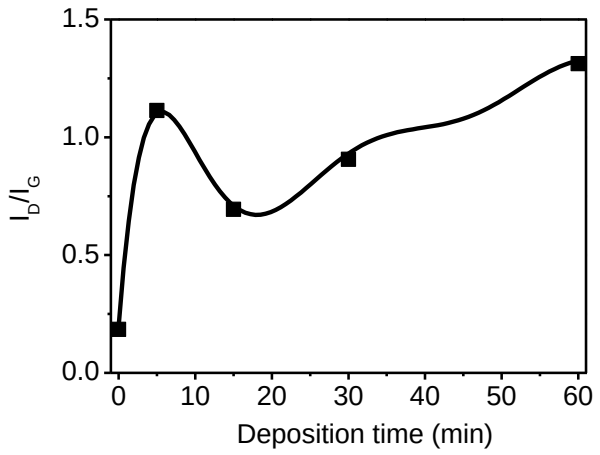

Fig. 5. I_D/I_G ratio of the different tungsten-doped diamond-like carbon films.

3.4 Film hardness

The mechanical properties of the tungsten-doped diamond-like carbon films are a key index for their use. The hardness was obtained by a nano-indentator with a maximum load of 600 nN and the loading/unloading rate was 2 nN/min. Since tungsten-doped diamond-like carbon films are relatively thin, the hardness measurements are a composite measure of the film and the substrate hardness. While the absolute values of the hardness may be different significantly, the relative changes found as a function of tungsten concentration are very similar. Fig. 6 presents the typical load-displacement and unload-displacement curves for different tungsten-doped diamond-like carbon films during the hardness test. No obvious crack and also no clear rubber effect were found. The hardness values at these loads more accurately reflected the hardness of the tungsten-doped diamond-like carbon films.

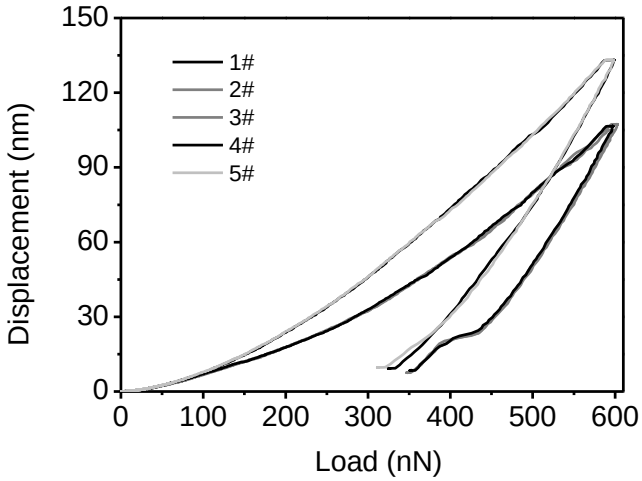

Fig. 6. Load-displacement and unload-displacement curves of the different tungsten-doped diamond-like carbon films.

It is known that the hardness is defined as [28]

$$H = \frac{P}{a_1 h_c^2 + a_2 h_c + a_3 h_c^{1/2} + a_4 h_c^{1/4} + \ldots} \quad (1)$$

where a_1, a_2, a_3, a_4 … are the adjustable constants of the diamond calibration coefficients, P is the applied load, the contact depth h_c is a function of the total displacement h_t and the elastic displacement h_e

$$h_c = h_t(1 - h_e/h_t) \quad (2)$$

The relationship is assumed to be valid for all depths h_t, and the h_e/h_t ratio is obtained from the initial portion of the unloading curve. Thus, h_c can be calculated from h_t and h_e by Eq. (2). Then, the hardness for different tungsten-doped diamond-like carbon films (See Fig. 7) can be obtained by Eq. (1). It can be seen that the hardness firstly enhances with the increasing of the indentation depth to a maximum value. Beyond the maximum, increasing of the indentation depth leads to a gradual decrease in hardness. For all tungsten-doped diamond-like carbon films, the hardness increases as a function of the tungsten deposition time and reaches a maximum value for sample 4. These results indicate that there is an optimal deposition time of tungsten which leads to the highest hardness. This hardness behavior may be due to the fact that the introduction of WC_{1-x} crystallites in the matrix, the collapses of sp^3 diamond-like matrix, and the change of sp^2-hybridized carbon domain.

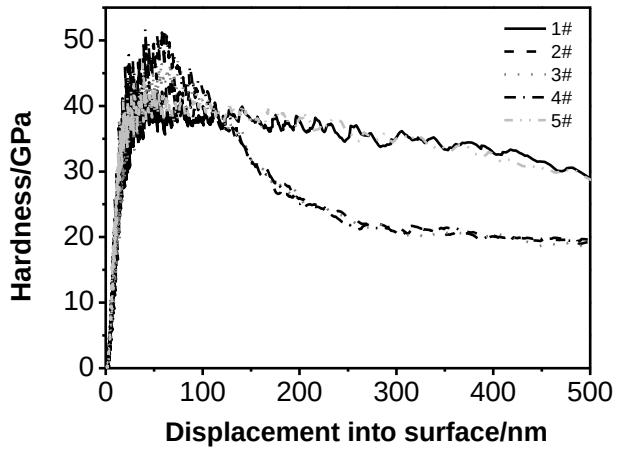

Fig. 7. Hardness of the different tungsten-doped diamond-like carbon films.

4. Conclusions

In summary, tungsten-doped diamond-like carbon films were deposited by pulsed-laser deposition method. The surface morphology and the structural, mechanical properties of the films depending on the incorporation of tungsten have been studied. The smooth surface of the films indicates their potential application in the tribological fields. Due to implantation of tungsten ions, the WC_{1-x} crystallites were produced in the films. The formation of WC_{1-x} crystallites in the matrix leads to the stress and hardness behaviors as a function of the tungsten deposition time.

Acknowledgements

Thanks for the supplied experiments and tests from Analytical and Testing center of Southwest University of Science and Technology.

References

[1] M. Pandey, D. Bhatacharyya, D.S. Patil, et al, Journal of alloys and compounds, **386**, 296 (2005).
[2] J. Roberton, Materials Science and Engineering R **37**, 129 (2002).
[3] V. Kn. Liechtenstein, T. M. Lvkova, E. D. Olshanski, et al, Nuclear Instruments and Methods in Physics Research Section A: Accelerators, Spectrometers, Detectors and Associated Equipment, **521**, 197 (2004).
[4] S. M. Chiu, S. C. Lee, C. H. Wang, F. C. Tai, et al, Journal of alloys and compounds, **449**, 379 (2008).
[5] A. C. Ferrari, J. Robertson, Physical Review B, 61, 14095 (2000).
[6] Hsin-Chung Cheng, Shi-Yung Chiou, Chung-Ming Liu, et al, Journal of alloys and compounds, **477**, 931 (2009).
[7] Carlos W. Mourae Silva, Jose R.T. Branco, Albano Cavaleiro, Solid State Sciences, **11**, 1778 (2009).
[8] Takanori Takeno, Hiroyuki Miki, Toshifumi, et al, Diamond and Related Materials, **17**, 713 (2008).
[9] E. Bertran, C. Corbella, A. Pinyol, et al, Diamond and Related Materials, **12**, 1008 (2003).
[10] B. Segura-Giraldo, E. Restrepo-Parra, P.J. Arango-Arango, Applied Surface Science, **256**, 136 (2009).
[11] Z. Q. Qi, E. I. Meletis, Thin Solid Films, **479**, 174 (2005).
[12] H. Ziegele, H. J. Scheibe, B. Schultrich, Surface and Coatings Technology, **97**, 385 (1997).
[13] D. M. Cao, B. Feng, W. J. Meng, et al, Applied Physics Letters, **79**, 329 (2001).
[14] B. Shi, W. J. Meng, L. E. Rehn, et al, Applied Physics Letters, **81**, 352 (2002).
[15] Wu Weidong, He Yingjie, Wang Feng, et al, Journal of Crystal Growth, **286**, 408 (2006).
[16] Wang Feng, Wu Weidong, Li Jun, et al, Science in China Series E: Technological Sciences, **52**, 850 (2009).
[17] M. D. Abad, J. C. Sánchez-López, N. Cusnir, et al. J. Appl. Phys. **105**, 033510-1 (2009).
[18] Y. Lifshitz, S. R. Kasi, J. W. Rabalais, et al, Physical Review B, **41**, 10468 (1990).
[19] J. F. Ziegler, Srim-2003, Nuclear Instruments and Methods in Physics Research Section B: Beam Interactions with Materials and Atoms, **219-200**, 1027 (2004).
[20] A. C. Ferrari, J. Robertson, Physical Review B, **61**, 14095 (2000).
[21] G. Irmer, A. Dorner-Reisel, Advanced Engineering Materials, **7**, 694 (2005).
[22] J. Schwan, S. Ulrich, V. Batori, H. Ehrhardt, S. R. P. Silva, Journal of Applied Physics, **80**, 440 (1996).
[23] Ai-Ying Wang, Kwang-Ryeol Lee, Jae-Pyoung Ahn, et al, Carbon, **44**, 1826 (2006).
[24] Ai-Ying Wang, Hyo-Shin Ahn, Kwang-Ryeol Lee, et al, Applied Physics Letters, **86**, 111902-1 (2005) .
[25] B. R. Pujada, F. D. Tichelaar, W. M. Arnoldbik, J. Appl. Phys. **105**, 033502-1 (2009).
[26] Xing-zhao Ding, B. K. Tay, S. P. Lau, et al, Thin Solid Films, **408**, 183 (2002).
[27] D. G. Mcculloch, S. Prawer, Journal of Applied Physics, **78**, 3040 (1995).
[28] Liuhe Li, Haiquan Zhang, Yanhua Zhang, et al, Materials Science and Engineering B, **94**, 95 (2002).

*Corresponding author: wuweidongding@163.com; wangxuemin75@sohu.com